PERGAMON

International Journal of Heat and Mass Transfer 45 (2002) 4333–4352

International Journal of HEAT and MASS TRANSFER

www.elsevier.com/locate/ijhmt

Temperature, velocity and mean turbulence structure in strongly heated internal gas flows Comparison of numerical predictions with data

Dariusz P. Mikielewicz [a,b], A. Mohsen Shehata [c], J. Derek Jackson [a], Donald M. McEligot [d,e,*]

[a] *Victoria University of Manchester, Manchester M13 9PL, UK*
[b] *Technical University of Gdansk, PL-80-952 Gdansk, Poland*
[c] *Xerox Corporation, Webster, New York, NY 14580, USA*
[d] *University of Arizona, Tucson, AZ 85721, USA*
[e] *Idaho National Engineering and Environmental Laboratory, P.O. Box 1625, Idaho Falls, ID 83415-3885, USA*

Received 19 March 2001; received in revised form 15 January 2002

Abstract

The main *objective* of the present study is to examine whether "simple" turbulence models (i.e., models requiring two partial differential equations or less for turbulent transport) are suitable for use under conditions of forced flow of gas at low Reynolds numbers in tubes with intense heating, leading to large variations of fluid properties and considerable modification of turbulence. Eleven representative models are considered. The ability of such models to handle such flows was assessed by means of computational simulations of the carefully designed experiments of Shehata and McEligot (IJHMT 41 (1998) 4297) at heating rates of $q^+_{in} \approx 0.0018$, 0.0035 and 0.0045, yielding flows ranging from essentially turbulent to laminarized. The *resulting* comparisons of computational results with experiments showed that the model by Launder and Sharma (Lett. Heat Transfer 1 (1974) 131) performed best in predicting axial wall temperature profiles. Overall, agreement between the measured velocity and temperature distributions and those calculated using the Launder–Sharma model is good, which gives confidence in the values forecast for the turbulence quantities produced. These have been used to assist in arriving at a better understanding of the influences of intense heating, and hence strong variation of fluid properties, on turbulent flow in tubes. Published by Elsevier Science Ltd.

1. Introduction

This paper is the second of a pair concerned with the low-Mach-number, turbulent flow of air upwards in a uniformly heated vertical circular tube, under conditions of *forced convection with significant fluid property variation*. The Reynolds number at the inlet to the tube is low (4260–6080) so that although the flow is initially turbulent it may become either partially or fully laminarized as a result of being heated [1,2]. The companion paper by Shehata and McEligot [3] provided the *first* data on mean *velocity* profiles for these conditions, along with mean temperature profiles, wall temperature distributions and axial pressure distributions in a carefully controlled experiment. Cooling by means of a gas is a problem which has already received considerable attention by virtue of its importance in gas turbine engines and rocket propulsion systems.

The use of a gas as a coolant in power generation systems and process heating offers a number of advantages. In particular, gases can be used at high temperature and this enables high thermal efficiencies to be achieved. By suitable choice of gas, advantage can be taken of chemical inertness, inherent safety and environmental acceptability. Consequently, helium and other gases are being considered as coolants for advanced power reactors, both fission and fusion. To obtain high

* Corresponding author. Address: Idaho National Engineering and Environmental Laboratory, P.O. Box 1625, Idaho Falls, ID 83415-3885, USA.

0017-9310/02/$ - see front matter Published by Elsevier Science Ltd.
PII: S0017-9310(02)00119-9

Nomenclature

$\{\}$	function of
A_{cs}	cross-sectional area
c_p	specific heat at constant pressure
D	tube diameter; term in dissipation equation
g	acceleration of gravity
g_c	units conversion factor, e.g., 1 kg m/(N s^2), 32.174 (lbm/lbf)/(ft/s^2), etc.
G	mean mass flux, $\dot{m}/A_{cs}$
h	convective heat transfer coefficient, $q''_w/(T_w - T_b)$; enthalpy
k	turbulent kinetic energy
l	mixing length; turbulent length scale
$\dot{m}$	mass flow rate
p	pressure
q''_w	wall heat flux
r	radial coordinate
R	tube wall radius
T	absolute temperature
u_τ	friction velocity, $(g_c \tau_w/\rho_w)^{1/2}$
v	local radial velocity component
V	time-mean radial velocity component
w	local streamwise velocity component
W	time-mean streamwise velocity component
W_b	bulk or mixed-mean streamwise velocity
x	axial coordinate measured from nominal start of heating
y	coordinate perpendicular to the wall
z	axial location

Non-dimensional quantities

B_j	buoyancy parameter, $Gr_q/(Re^{3.425}Pr^{0.8})$
f	friction factor, $2\rho_b g_c \tau_w/G^2$
Gr_q	local Grashof number based on heat flux, $gD^4 q''_w/(v_b^2 \lambda_b T_b)$
K_v	acceleration parameter, $(v/W_b^2)(dW_b/dx)$
Nu	local Nusselt number, e.g., hD/λ
P^+	local pressure defect, $\rho_{in} g_c (p_{in} - p)/G^2$
Pr	Prandtl number, $c_p \mu/\lambda$
q^+	heat flux parameter, q''_w/Gc_pT; q_i^+, based on inlet conditions, $q''_w/Gc_{p,in}T_{in}$
R	turbulence Reynolds number, in Wolfshtein model
Re	Reynolds number, $4\dot{m}/\Pi D\mu$
u^+	streamwise velocity component, W/u_τ
y^+	wall distance coordinate, $y(g_c \tau_w/\rho_w)^{1/2}/\nu_w$

Greek symbols

δ	effective viscous layer thickness
δ^+	viscous layer thickness in wall coordinates, $\delta(g_c \tau_w/\rho_w)^{1/2}/\nu_w$; δ_{M^+}, in velocity profile; δ_{T^+}, in temperature profile for buoyancy analysis; δ_{H^+}, in temperature profile for acceleration analysis
ε	dissipation of turbulence kinetic energy; $\bar{\varepsilon}$, isotropic dissipation function, $\varepsilon - D$
λ	thermal conductivity
μ	absolute viscosity; μ_t, turbulent viscosity
ν	kinematic viscosity, μ/ρ
ρ	density
σ	turbulent Prandtl number, e.g., σ_t, for thermal energy
τ	shear stress; turbulent time scale; τ_w, wall shear stress
ω	specific dissipation rate

Subscripts

b	evaluated at bulk or mixed-mean temperature (or enthalpy)
cp	constant property idealization
fc	for forced convection
i, in	inlet, inner
t	turbulent
w	wall, evaluated at wall temperature

Miscellaneous constants and functions in turbulence models are defined as used

thermal efficiencies, gas flow rates may be kept relatively low to give high outlet temperatures. For example, at the exit of the cooling channels in Japan's High Temperature Engineering Test Reactor the design Reynolds number is about 3500.

The general effects of intense heating of a gas are variation of the transport properties, reduction of density causing acceleration of the flow in the central core and, under some conditions, significant buoyancy forces. Growth of the internal thermal boundary layer leads to readjustment of the flow. With an imposed wall heat flux distribution, truly fully established conditions will not be reached because the temperature rises leading, in turn, to continuous axial and radial variation of fluid properties such as the viscosity, thermal conductivity and density.

In the present paper the term "moderate heating" is used to describe conditions where the property variation is significant but turbulent heat transfer parameters may be predicted adequately using an appropriate *variable properties* turbulent correlation equation. Typically, such equations are valid up to local temperature ratios T_w/T_b of about 2.5 (or non-dimensional heating rates q^+ of about 0.003) [4]; however, these limits vary with Reynolds number. Beyond these levels we would refer to the conditions as representing "intense heating" and expect strong influences on turbulence and heat transfer

behavior which would not be adequately described by simple equations.

The non-dimensional heating rate $q^+_{in} = q''_w/Gc_{p,in}T_{in}$ evolves naturally from non-dimensionalizing the governing equations and boundary conditions in pipe flow with an imposed wall heat flux distribution [5]. Property effects come in via the (non-dimensional) exponents in the power law representations. This parameter is directly related to the rate of increase of the bulk temperature and the wall-to-bulk temperature ratio. The parameter q^+ is also directly related to the acceleration parameter K_v, used by Kline et al. [6] as an indicator of the likelihood of laminarization occurring in external boundary layers, as $K_{v,in} \approx 4q^+_{in}/Re_{in}$ [7]; further insight on this aspect is provided later in the section dealing with the influences of intense heating on turbulence.

Turbulence models have generally been developed for conditions approximating the constant properties idealization. The few "advanced" turbulence models applied for high heating rates [8–11] were developed without the benefit of velocity and temperature distributions in strongly heated, dominant forced flow for guidance or testing. Thus, it is not certain whether the agreement with wall temperature data for moderate and strong wall heat fluxes, that was obtained in some cases with such models, was fortuitous or not. Before they can be applied with confidence to gas-cooled systems with high heat fluxes, turbulence models must be validated by comparison of predictions with careful measurements of the mean flow and thermal fields for conditions with significant gas property variation.

It would appear that until Shehata [12] obtained his mean velocity distributions for *dominant forced convection with significant gas property variation*, in low-Mach-number gas flow through a circular tube, the only published profile data available to test predictive turbulence models for that situation were the measurements of mean temperature distributions by Perkins [2]. The experiments of Shehata and of Perkins were conducted using an open flow system incorporating a vertical, resistively heated, circular test section exhausting directly to the atmosphere in the laboratory. The experiment was designed to provide an approximately uniform wall heat flux boundary condition in a tube for ascending air entering with a fully developed turbulent velocity profile at a uniform temperature. The heated length was kept relatively short to permit high heating rates with Inconel as the material while possibly approaching quasi-developed conditions. Small single wire probes were introduced through the open exit in order to obtain pointwise temperature and velocity measurements. In addition to the usual difficulties of hot wire anemometry, the temperature range of his experiment introduced additional problems such as radiation corrections; these difficulties, their solutions and related supporting measurements are described by Shehata [12] and Shehata and McEligot [13]. Shehata's careful measurements are now readily available [3] and can be used to provide a further basis for evaluation of turbulence models for these conditions. Inlet Reynolds numbers ($Re_{in} = 4\dot{m}/(\Pi D\mu_{in})$) of ≈6000 and 4000 were employed and attention was concentrated on three heating rates chosen to give significant variation of properties for conditions of predominantly forced convection which were considered to be "turbulent", "intermediate" and "laminarizing", respectively ($q^+_{in} \approx 0.0018$, 0.0035 and 0.0045).

The main *objective* of the computational study reported here was to examine whether computational simulations modeling a variety of simple turbulence models could reproduce the integral heat transfer behavior and the internal velocity and temperature distributions found in the experiment referred to above. Another objective was to throw light on the mechanisms by which extreme property variations due to intense heating can cause impairment of heat transfer through the laminarization of turbulent flow. The models employed ranged from mixing length models and eddy diffusivity models to models with one governing equation for turbulence (k), k–ε models with low-Reynolds-number treatments and two-equation models with alternative turbulence variables that can be converted to k–ε models. The scope of the present study was limited to such models to avoid treatments which would be more difficult for a thermal engineer to apply to practical problems.

After presenting the governing equations and boundary conditions, we identify the turbulence models examined and the numerical technique used. The first assessment is by comparison to a simple idealization, fully established flow with constant fluid properties; this test immediately eliminated most models. Predictions of integral results and mean velocity and temperature distributions are examined next by comparison to the data of the companion paper [3], mentioned above. The final section is devoted to further discussion of the numerical results, including consideration of the mechanisms by which property variations and buoyancy lead to impairment of heat transfer. Finally, a summary of the main observations is presented by way of concluding remarks. Further details of the experiments are available in the reports by Shehata [12] and Shehata and McEligot [13] with (slightly) revised tabulations in the latter report. The numerical simulations are reported in detail in the thesis of Mikielewicz [14].

Consequently, new knowledge provided by the present paper includes the confirmation that a model(s) can be directly extended to simulate the internal mean distributions of strongly heated flows usefully, insight into the effects leading to laminarization and how they relate to the model(s) and observation of the behavior of the simulated turbulent shear stress which leads to validated predictions of internal velocity and temperature fields.

2. Computational technique

2.1. Governing equations

The theoretical formulation and calculation procedures used in this study follow those of Cotton [15]. The conditions considered are those of steady, single-phase, axisymmetric flow in a vertical tube with no swirl and no flow reversal. The governing equations are cast in the "internal boundary layer" approximation which reduces significantly the number of terms appearing in the conservation equations and permits numerical solution by a "marching" technique. Modifications to the formulation which take account of the temperature dependencies of the thermodynamic and transport properties made by Yu [16] and Mikielewicz [14] are incorporated.

The mean flow equations for conservation of mass, momentum and thermal energy are written in the "thin shear layer" form, which results from considering flow where there is a clear principal flow direction and the principle variation of velocity occurs in the direction normal to this direction. In the duct geometry considered, a circular tube, the principal flow direction coincides with the axis. These governing equations become

Continuity equation

$$\frac{1}{r}\frac{\partial(\rho r V)}{\partial r}+\frac{\partial(\rho W)}{\partial z}=0$$

Momentum equation

$$\frac{1}{r}\frac{\partial(r\rho VW)}{\partial r}+\frac{\partial(\rho W^2)}{\partial z}=-\frac{\mathrm{d}p}{\mathrm{d}z}+\frac{1}{r}\frac{\partial}{\partial r}\left[r(\mu+\mu_{\mathrm{t}})\frac{\partial W}{\partial r}\right]+\rho g$$

Energy equation

$$\frac{1}{r}\frac{\partial(r\rho Vh)}{\partial r}+\frac{\partial(\rho Wh)}{\partial z}=\frac{1}{r}\frac{\partial}{\partial r}\left[r\left(\frac{\lambda}{c_p}+\frac{\mu_{\mathrm{t}}}{\sigma_{\mathrm{t}}}\right)\frac{\partial h}{\partial r}\right]$$

For the two-equation turbulence models, the equations used to describe the transport of turbulence kinetic energy and its rate of dissipation become

k-transport

$$\frac{1}{r}\frac{\partial(\rho r Vk)}{\partial r}+\frac{\partial(\rho Wk)}{\partial z}=\mu_{\mathrm{t}}\left(\frac{\partial W}{\partial r}\right)^2+\frac{1}{r}\frac{\partial}{\partial r}\left[r\left(\mu+\frac{\mu_{\mathrm{t}}}{\sigma_k}\right)\frac{\partial k}{\partial r}\right]-\rho\varepsilon+\rho\Pi$$

ε-transport

$$\frac{1}{r}\frac{\partial(\rho r V\varepsilon)}{\partial r}+\frac{\partial(\rho W\varepsilon)}{\partial z}=C_1 f_1\frac{\varepsilon}{k}\mu_{\mathrm{t}}\left(\frac{\partial W}{\partial r}\right)^2+\frac{1}{r}\frac{\partial}{\partial r}\left[r\left(\mu+\frac{\mu_{\mathrm{t}}}{\sigma_\varepsilon}\right)\frac{\partial\varepsilon}{\partial r}\right]-C_2 f_2 f_3\frac{\rho\varepsilon^2}{k}+\rho E$$

The various two-equation models examined in this study differ in respect of the form of the functions f_μ, f_2 and f_3 which are used and the additional terms Π and E introduced to account for pressure diffusion of k and production of ε, respectively, in the near-wall region. Instead of using $k^{3/2}/\varepsilon$ as a turbulence length scale, some models use $k^{3/2}/\bar{\varepsilon}$, in which $\bar{\varepsilon}=\varepsilon-D$, the form of the function D being chosen so that the isotropic dissipation function $\bar{\varepsilon}$ takes the value zero at the wall. The dissipation equation is then usually (but not always) solved for $\bar{\varepsilon}$ instead of ε. To account for effects of buoyancy, the body force term appears in the source term of the momentum equation but buoyancy effects are not included in the transport equations for turbulent energy and dissipation rate. The significance of buoyancy forces is discussed later.

The integral continuity equation, a statement of conservation of the mass flow rate $\dot{m}$, is the final equation relating the dependent variables, W, V, h, k, ε and p. It takes the form

$$\dot{m}=2\Pi\int\rho Wr\,\mathrm{d}r$$

(The dependent variables comprise five two-dimensional quantities and one that is one-dimensional, p; consequently, the mathematical statement requires five partial differential equations and one integral equation to be described fully.)

For the flow—the condition of no-slip is applied at the tube wall, which is assumed to be impermeable and it is assumed to be symmetrical about the centerline. For the equation representing dissipation of turbulence, the wall boundary condition differs between the various turbulence models, as indicated in the next section. The thermal condition at the wall is a specified axial distribution of wall heat flux; in the experiments considered, it (approximately) shows an exponential approach to a near-uniform value in a few diameters. The governing partial differential equations form a parabolic set and the initial conditions imposed are specified fully developed profiles of the streamwise velocity, turbulence kinetic energy and dissipation and a uniform temperature profile. Preliminary calculations for an unheated tube were performed to generate these profiles, starting with approximate assumed profiles; invariant conditions were obtained within about 60 diameters.

All fluid properties are taken as temperature dependent. Thermal conductivity, dynamic viscosity and specific heat are calculated using relations for air due to Wisniewski [17], in the form of polynomials of temperature. The perfect gas approximation is used to describe the temperature dependence of density.

2.2. Turbulence models examined

For general background on turbulence modeling, the reader is referred to introductory materials in the texts by Launder and Spalding [18] or Kays and Crawford

[19] plus the publications of the authors cited in the case of the turbulence models used here, which are

ML	Mixing length (Nikuradse [20], van Driest [21])
RC	Prescribed eddy diffusivity (Reichardt [22])
DS	Implicit eddy diffusivity (Deissler [23])
WA	One-equation k (Wolfshtein [24], Axcell and Hall [25])
JL	Low-Reynolds-number k–ε (Jones and Launder [26,27])
LS	Low-Reynolds-number k–ε (Launder and Sharma [28])
CH	Low-Reynolds-number k–ε (Chien [29])
LB	Low-Reynolds-number k–ε (Lam and Bremhorst [30])
MRS	Low-Reynolds-number k–ε (Michelassi et al. [31])
SH	Low-Reynolds-number k–ε (Shih and Hsu [32])
TAS	Low-Reynolds-number k–τ (Thangam et al. [33])

With a few exceptions as noted below, the models were used in the form described in the publications cited above. For the two-equation models, the model constants and functions employed are listed in Tables 1 and 2 and the extra terms and model features are given in Tables 3 and 4, respectively. As noted in Section 1, the scope of the present investigation is constrained to two-equation models so Reynolds stress models were not considered. If a two-equation model is found that simulates the internal mean velocity and temperature fields reasonably, there is not a significant incentive to use more complicated models for the purposes of the present study. As shown by Torii and colleagues [10], a Reynolds stress model does not necessarily do well for "intermediate" conditions. In a parallel investigation during the preparation of the present paper, Nishimura [34] has apparently applied a Reynolds stress model to simulate the data of Shehata and McEligot [13] successfully.

In all cases, a value of 0.9 was chosen for the turbulent Prandtl number σ_T; this approach is a popular means of avoiding complicating the calculations further. While there is evidence from direct numerical simulations [35] that σ_T may vary with y^+ (and Pr), Bankston and McEligot [5], McEligot and Bankston [36] and successors have successfully employed constant turbulent Prandtl numbers to simulate data with large temperature gradients and property variation. The companion paper [3] is an example. Part of the reason for such success is the dominance of the thermal resistance in the viscous layer as opposed to the central core of a heated flow; large variations in σ_T will not cause a significant effect on the temperature distribution since the thermal resistance of the core region is already low [37]. More complicated treatments of the thermal transport, such as solution of additional equations for turbulent heat flux, do not necessarily provide better simulations even for simpler flows with constant properties as shown by Ezato et al. [38] and Torii and Yang [11, Figs. 2 and 5].

In the case of the mixing length model, the Nikuradse [20] distribution was combined with the van Driest [21] wall damping function in order to examine a nearly original version. The van Driest model has been extended by McEligot and Bankston [36] to handle low-Reynolds-number turbulent and laminarizing flows; simulations with this modified version have been presented in the companion paper [3].

The one-equation model of Wolfshtein [24] was used in the form modified by Axcell [39] (see Axcell and Hall [25]) to apply to "fully developed" pipeflow by revising the original constants. The equation for turbulence kinetic energy in the "modified Wolfshtein model" is

$$\frac{1}{r}\frac{\partial(\rho r V k)}{\partial r}+\frac{\partial(\rho W k)}{\partial z}=\mu_t\left(\frac{\partial W}{\partial r}\right)^2+\frac{1}{r}\frac{\partial}{\partial r}\left[r\left(\mu+\frac{\mu_t}{\sigma_k}\right)\frac{\partial k}{\partial r}\right]-\frac{C_D\rho k^{3/2}}{l_D}$$

where $\mu_t=C_\mu\rho k^{1/2}l_\mu$, $R=k^{1/2}y/\nu$, $l_\mu=y[1-\exp\{-A_\mu R\}]$ and $l_D=y[1-\exp\{-A_D R\}]$. The quantities C_μ and C_D are empirical constants and l_μ and l_D are length scales for turbulent diffusion and dissipation, respectively. The constants are assigned the values $C_\mu=0.09$, $C_D=0.09$, $\sigma_k=1.0$, $A_\mu=0.0173$ and $A_D=0.205$ here.

Wilcox [40] suggested that k–ε models have shortcomings for boundary layer flows and proposed instead using ω, a specific dissipation rate, as the dependent

Table 1
Model constants

Model	C_μ	C_1	C_2	σ_k	σ_ε
LS	0.09	1.44	1.92	1.0	1.3
JL	0.09	1.55	2.0	1.0	1.3
Chien	0.09	1.35	1.8	1.0	1.3
LB	0.09	1.44	1.92	1.0	1.3
SH	0.09	1.5	2.0	1.3	1.3
MRS	0.09	1.44	1.92	1.3	1.3
TAS	0.096	1.44	1.83	1.36	1.36

Table 2
Damping functions

Model	f_μ	f_2
LS	$\exp(-3.5/(1+Re_t/50)^2)$	$1-0.3\exp(-Re_t^2)$
JL	$\exp(-2.5/(1+Re_t/50))$	$1-0.3\exp(-Re_t^2)$
Chien	$1-\exp(-0.0115y^+)$	$1-0.22\exp(-Re_t^2/36)$
LB	$[1-\exp(-0.0165Re_y)]^2\left(1+\frac{20.5}{Re_t}\right)$	$1-\exp(-Re_t^2)$
SH	$1-\exp(-a_1Re_w^{1/4}-a_2Re_w^{1/2}-a_3Re_w)$ where $a_1=5\times10^{-3}$, $a_2=7\times10^{-5}$, $a_3=8\times10^{-7}$	$\left[1-0.22\exp\left(-\frac{Re_t^2}{36}\right)\right]\frac{\tilde{\varepsilon}}{\varepsilon}$
MRS	$\frac{[1-\exp(-0.044y^+)]^2}{1+6\exp(-0.12y^+)}$	$\left[1-0.22\exp\left(-\frac{Re_t^2}{36}\right)\right]\frac{\tilde{\varepsilon}}{\varepsilon}$
TAS	$(1+3.45/Re_t^{1/2})\tanh(y^+/70)$	$[1-\exp(-y^+/4.9)]^2[1-0.22\exp(-Re_t^2/36)]$

Note: $f_1=f_3=1$ in all models except $f_1=1+(0.05/f_\mu)^3$ in LB and $f_3=\exp(2.1Re_p^3)$ in MRS.

Table 3
Extra terms

Model	D	E
LS	$2\nu\left(\frac{\partial\sqrt{k}}{\partial y}\right)^2$	$2\nu\nu_t\left(\frac{\partial^2W}{\partial y^2}\right)^2$
JL	$2\nu\left(\frac{\partial\sqrt{k}}{\partial y}\right)^2$	$2\nu\nu_t\left(\frac{\partial^2W}{\partial y^2}\right)^2$
Chien	$-2\nu k/y^2$	$-\frac{2\nu\varepsilon}{y^2}\exp(-0.5y^+)$
LB	0	0
SH	$\varepsilon\exp(-Re_t^{1/2})$	$2\nu\nu_t\left(\frac{\partial^2W}{\partial y^2}\right)^2$
MRS	$\varepsilon\exp(-0.09Re_y)$	$1.2\nu\nu_t(\partial^2W/\partial y^2)^2+0.0085\nu\frac{k}{\varepsilon}\frac{\partial k}{\partial y}\frac{\partial W}{\partial y}\frac{\partial^2W}{\partial y^2}$
TAS	0	0

Note: $\Pi=0$ in all the models except in SH where $\Pi=\frac{1}{r}\frac{\partial}{\partial y}\left(r\frac{0.01}{f_\mu^2}\frac{\nu_t}{\sigma_k}\frac{\partial k}{\partial y}\right)$.

Table 4
Model features

Model	Dissipation equation	BC for ε at wall	Length scale	Asymptotic feature of ν_t	Parameters used in f_μ
LS	$\tilde{\varepsilon}$	$\tilde{\varepsilon}=0$	$k^{3/2}/\tilde{\varepsilon}$	$0(y^3)$	Re_t
JL	$\tilde{\varepsilon}$	$\tilde{\varepsilon}=0$	$k^{3/2}/\tilde{\varepsilon}$	$0(y^3)$	Re_t
Chien	$\tilde{\varepsilon}$	$\tilde{\varepsilon}=0$	$k^{3/2}/\tilde{\varepsilon}$	$0(y^3)$	y^+
LB	ε	$\partial\varepsilon/\partial y=0$ or $\varepsilon=\frac{\nu\partial^2k}{\partial y^2}$	$k^{3/2}/\varepsilon$	$0(y^4)$	Re_y & Re_t
SH	ε	$\varepsilon=2\nu\left(\frac{\partial\sqrt{k}}{\partial y}\right)^2$	$k^{3/2}/\tilde{\varepsilon}$	$0(y^3)$	Re_w
MRS	ε	$\varepsilon=2\nu\left(\frac{\partial\sqrt{k}}{\partial y}\right)^2$	$k^{3/2}/\tilde{\varepsilon}$	$0(y^3)$	y^+
TAS	ε	$\varepsilon=2\nu\left(\frac{\partial\sqrt{k}}{\partial y}\right)^2$	$k^{3/2}/\tilde{\varepsilon}$	$0(y^3)$	Re_t & y^+

Note: $Re_t=\frac{k^2}{\nu\varepsilon}$, $Re_y=\frac{\sqrt{k}y}{\nu}$, $y^+=\frac{u_\tau y}{\nu}$, $Re_w=\frac{W^4}{\nu\varepsilon}$ and $Re_p=\frac{\nu_t(\partial W/\partial y)^2}{k\sqrt{C_\mu\varepsilon/\nu}}$.

variable for the second turbulence transport equation. The physical interpretation of ω is that it is the ratio of the dissipation rate ε to turbulent mixing energy. Although the model does not include damping functions to account for wall proximity effects, it is of a form that can be integrated directly to the wall rather than using a wall function. Thangam et al. [33] proposed that, by using a turbulent time scale, $\tau = 1/\omega$, with wall damping functions having improved asymptotic behavior, the shortcomings of both the k–ε and k–ω formulations could be alleviated. Their argument was that the k–τ model possesses a natural boundary condition near the wall that is lacking for ε. For the purpose of the present numerical simulations, the τ equation was converted to an equation for ε.

From the condition of no slip, the wall boundary condition for turbulence kinetic energy is $k = 0$. For turbulence dissipation rate, the various authors use a variety of versions depending on the physical bases of their models. In the present simulations, the wall boundary conditions for the ε equation were evaluated as shown in Table 4.

2.3. Numerical method

The computer program, used in the study reported here, is a version of the "CONVERT" code initially developed by Cotton [15] and later extended by Yu [16] and Mikielewicz [14]. The differential equations are discretized using a finite-control-volume formulation following the approach of Leschziner [41]. The resulting algebraic equations are decomposed into two bi-diagonal matrices and are later solved using the Gaussian-elimination method. Since the set of partial differential equations is parabolic in character, the solution is obtained by starting with specified distributions of the dependent variables at the inlet and proceeding in steps downstream. At each downstream station, the equations are solved iteratively to take account of the non-linearities and strong coupling.

Non-uniform distributions are employed for the node spacing in both radial and axial directions. A fine grid is needed in the near wall region to resolve steep gradients in the mean and turbulence fields; a procedure developed by Cotton [15] is used to generate the spacing. In the radial direction, 101 nodes are assigned with the first at $y^+ = 0.5$ and the 51st at $y^+ \approx 30$. In the streamwise direction step sizes are based on $\Delta z^+ \approx 10$, i.e., about two "linear" layer thicknesses.

Property values are recalculated at all nodal positions and control volume faces as appropriate at each iteration. The streamwise pressure gradient is determined iteratively to satisfy the overall continuity equation [42]; the estimated value is adjusted until the calculated mass flow rate agrees with the specified total mass flow rate. Under-relaxation was introduced in the iterative process; a relaxation factor of 0.05 was applied to the k and ε fields for the second and subsequent iterations at each axial station. Typically, the solution was taken as converged at a station when the normalized changes between successive iterations decreased to 10^{-6} for the velocity field and to 10^{-4} for turbulence kinetic energy. For further details concerning the numerical procedure, the reader is referred to the theses of Mikielewicz [14], Yu [16] and Cotton [15].

Numerical accuracy of the calculation procedure has been examined by Cotton [15], Yu [16] and Kirwin [43] by conducting sensitivity tests and making comparisons with accepted results. Simulations of mixed and forced convection have been examined for low and high Reynolds numbers and for constant and variable properties. The sensitivity tests involved varying radial and axial spacing of nodes, convergence criteria, relaxation factors and number of iterations of the thermal energy equation. With a less stringent constraint for the velocity solution, when changing the relaxation factor from 0.2 to 0.05 Kirwin found an increase of $\approx$2% in Nusselt number. In general, criteria more stringent than those used in the present study (halving or doubling, as appropriate) changed parameters, such as Nusselt number, friction factor and centerline velocity, $<$0.1%.

3. Constant properties predictions

One would want both heat and momentum transfer to be handled adequately for constant properties before treating cases with property variation; this section considers both. This initial consideration of a case with heat flux uses the constant properties idealization so the flow and momentum transfer are equivalent to adiabatic conditions. As an initial assessment of the turbulence models examined in the present study for use at low-Reynolds-number flows, calculations were made for fully developed flow and heat transfer to air in a uniformly heated tube to determine friction factor and Nusselt number with the constant properties idealization. The Prandtl number used was 0.7 and the Reynolds number range covered was $4000 < Re < 60{,}000$. To obtain constant property heat transfer predictions, the calls to the property subroutines were suppressed and properties were held constant at the initial values throughout the calculation (consequently, the results become independent of the value of q^+ used for the calculation or, in a sense, equivalent to $q^+ \approx 0$). To obtain results for the fully established flow and heat transfer idealization, the heat transfer calculations were started with the approximate flow profiles at the inlet and were continued for 100 diameters from the start of heating to achieve fully developed flow and thermal conditions. Predicted values of friction factor and Nusselt number at the outlet obtained using the various

Table 5
Calculations of friction factors (f/f_{Blasius}) for fully developed flow at constant properties

Re	ML	WA	JL	SH	CH	TAS	LS
4280	1.097	1.170	1.213	1.123	1.024	1.070	0.944
6060	0.932	1.106	1.182	1.075	0.958	1.038	0.930

turbulence models are compared in Table 5 and Fig. 1, respectively, to those given by accepted empirical equations for turbulent flow in the low-Reynolds-number range. The empirical equation used for friction coefficients is the Blasius equation.

With the idealizations of fully developed flow and constant properties, the predictions of friction factor at the Reynolds numbers of interest here gave results that are mostly high relative to the Blasius correlation. The friction factors presented in Table 5 are for the inlet conditions of Shehata's experiment, i.e., $Re \approx 4280$ and 6060 for the CH, JL, LS, ML, SH, TAS and WA models. Closest to the Blasius equation values are the predictions from the CH, LS and TAS models. The other four models forecast discrepancies of about 10% or more. These discrepancies are not surprising. Launder and Priddin [44] earlier demonstrated in a more limited manner that some turbulence models do not do well for predicting the friction factor in pipeflow (their Fig. 3). Patel et al. [45] showed that some popular turbulence models do not even predict skin friction coefficients well for a flat plate boundary-layer at high Reynolds numbers. A low-Reynolds-number pipe flow requires a significant favorable streamwise pressure gradient (in non-dimensional terms). Patel et al. found that only a few models predicted $c_f\{x\}$ reasonably for a turbulent boundary layer with a significant favorable streamwise pressure gradient.

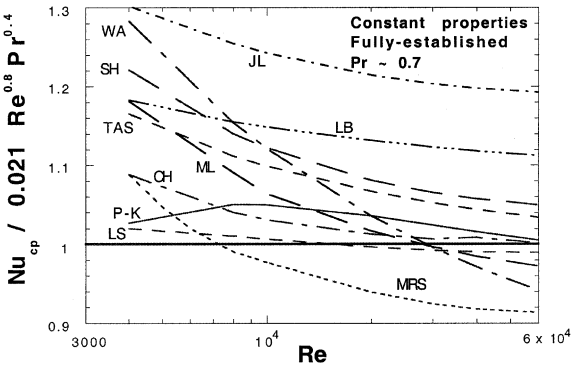

Fig. 1. Low-Reynolds-number predictions for fully established flow in a circular tube with constant properties from various turbulence models [14] normalized by Dittus–Boelter [46] correlation. Curve labeled P–K is an accepted empirical correlation by Petukhov et al. [49].

For Nusselt number, the Dittus–Boelter equation [46], with the coefficient taken as 0.021 [8,47], was employed for comparison purposes. McEligot et al. [48] showed that for common gases that equation is valid to within about 5% for $Pr \approx 0.7$ and Reynolds numbers greater than about 2500. This relation is the basis of the normalization in Fig. 1. Also shown is the relation proposed by Petukhov et al. [49]; this is claimed to fit available data for the ranges $4000 < Re < 6 \times 10^5$ and $0.7 < Pr < 5 \times 10^5$ to within about 4%. Based on the predictions of Nusselt number, several popular models could be immediately eliminated from further consideration. The JL, LB and WA models do not even handle high-Reynolds-number flows well for heat transfer in a simple circular tube. The Reichardt, Deissler and van Driest/Nikuradse models were all essentially developed for use with higher Reynolds numbers than those which are of interest here in conjunction with simulation of intensively heated pipe flow with strong variation of fluid properties (see later section). No modifications have been made to account for effects that become important at low Reynolds number. Consequently, the Nusselt numbers predicted using these models diverge from the values given by the empirical correlations as the Reynolds number is reduced. At $Re = 5000$, predictions using the Reichardt eddy diffusivity model were some 40% higher than the Dittus–Boelter value. The Deissler model gave results over 25% high. The predictions of the van Driest/Nikuradse model were much nearer (only about 15% high at $Re = 5000$).

Several k–ε models designed for use at low Reynolds number also gave poor results. At $Re = 5000$, the value obtained using the Jones and Launder model was over 30% high and the Lam and Bremhorst and the Shih and Hsu predictions were over 15% high. The low-Reynolds-number k–τ model of Thangam et al. was about 14% high. The only model which gave acceptable results was that of Launder and Sharma; its predictions fell within the estimated experimental uncertainties of the empirical values. The Chien version was slightly high at low Reynolds numbers (about 8%) and the Michelassi et al. version was about 8% low at high Reynolds numbers.

4. Comparisons to experiments with strong heating

To assess the potential of turbulence models to handle difficult conditions with significant property variation for common gases, calculations have been

made for air using several models simulating the experiment of Shehata. His very careful study has been described in the companion paper [3]; further details are provided in the report by Shehata and McEligot [13] and the theses of Perkins [2] and Shehata [12]. Inlet Reynolds numbers used were about 6080 and 4260 with non-dimensional heating rates, $q^+ = q''_w/(Gc_pT_i)$, of about 0.0018, 0.0035 and 0.0045 yielding a range of flows from essentially turbulent to laminarizing. For ease of reference to the reader, these conditions are called Runs 618, 635 and 445 (i.e., the first digit represents the inlet Reynolds number and the last two indicate the heating rate). Over the range $5 < x/D < 26$ the wall heat flux was uniform to within about 3% of the average value. The test section provided a path for thermal conduction in the upstream direction and also thermal radiation; consequently, there was some slight preheating of the flowing gas (discussed later). Based on consideration of non-dimensional buoyancy parameters and evidence to be discussed later, it was concluded that buoyancy effects on the heat transfer results would have been slight to negligible.

In the calculations to simulate these flows with significant property variation, the flow profiles at the entry were obtained from computational predictions of fully developed, isothermal flow at the measured mass flow rate for each turbulence model. The inlet pressure and temperature were set to the measured values. Shehata and McEligot [13] presented the wall temperatures upstream from the first electrode in the region affected by upstream thermal conduction; the simulations were made using a distribution of wall heat flux to correspond to these tabulated temperatures in the first 14.8 diameters matched to Shehata's deduced heat flux distribution for the electrically heated region.

To illustrate the predictions of integral heat transfer, Fig. 2 presents the resulting wall temperature distributions for eight models for the three runs. For the thermal design engineer, these are of key importance. (If desired, approximate non-dimensional temperatures may be obtained by converting to the Kelvin scale and dividing by an entry temperature of about 297 K.) In this figure the distance z/D is labeled from the start of the calculation, so the nominal start of heating is at $z/D \approx 14.8$ and the near-uniform wall heat flux range is in the region $20 < z/D < 41$. End conduction effects and radiation to the open exit of the test section reduce the wall heat flux and wall temperatures beyond $z/D \approx 41$. The expected sharp rise of wall temperature after the abrupt increase in wall heat flux (near $z/D = 15$) is demonstrated by all the models. All show the expected decrease in wall temperature as the heat flux falls at the end of the test section (not shown).

In Fig. 2 the identification of the models is via the letter labels assigned earlier, e.g., LS, TAS, etc. The symbols are the measurements from Shehata [12]. For

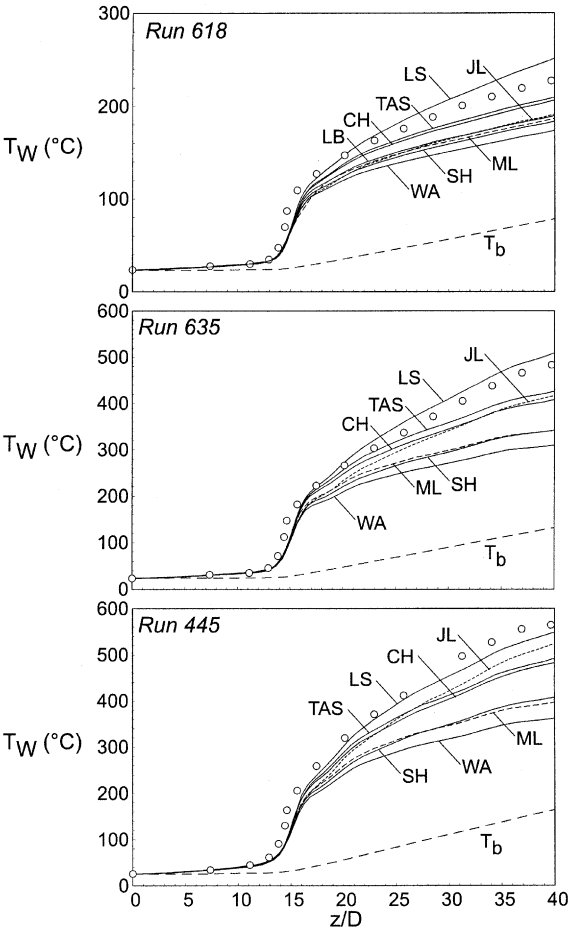

Fig. 2. Predicted local wall temperatures (lines) compared to measurements (circles) of Shehata [12].

the lowest heating rate, "turbulent" run 618, the trends from model to model are approximately the same as for the results for fully established heat transfer with constant properties that were presented in Fig. 1; models which did not reproduce that condition well predict the behavior with property variation poorly as well. For the purpose of making quantitative comparisons, we examine the predictions at $z/D \approx 40$ where the wall temperature is highest. The wall-to-bulk temperature difference is underpredicted by over 40% in the worst case. The discrepancy is 30% in the case of one "low-Reynolds-number" k–ε model (SH), actually slightly worse than the high-Reynolds-number mixing length model. The low-Reynolds-number k–ε models of Jones and Launder and of Lam and Bremhorst gave approximately the same results as the mixing length model. Forecasts within 20% of the measured values were yielded by Michelassi et al., by Chien and by Thangam et al. The model of Launder and Sharma did slightly better with a conservative overprediction of about 13%.

Comparisons in the cases of the two higher heating rates discriminate amongst the models further. In general, the models showing poor agreement at the lower heating rate remained poor. Numerical difficulties were experienced using a couple models when they were applied under conditions of strongly varying properties and no results were produced. The one-equation model underpredicted the temperature difference by 55% or more for such conditions.

There were some differences in relative rankings of the models as the heating rate was increased and Reynolds number decreased. The LS model clearly performed best in each case. The SH model improved slightly compared to the mixing length predictions but both underpredicted by up to about 40%. The JL model improved relative to the CH and TAS low-Reynolds-number k–ε models. At the lower Reynolds number, as one might expect, some of the low-Reynolds-number k–ε models performed better in comparison to the van Driest mixing length model which was developed for high Reynolds number flows.

The distributions of local Nusselt number are compared with the data in Fig. 3; the labels used are as in Fig. 2 and the earlier list. Near the start of heating, the apparatus consists of the continuous tube as a test section with a thin circular electrode joined to its outside surface; this region is surrounded by granular insulation and then a shield with guard heating [2]. The resulting distribution of heat flux to the flowing air is difficult to deduce precisely in the immediate vicinity of this electrode [1, Appendix C] so its experimental uncertainties are greater in this region. Also numerical results become more uncertain in the vicinity of abrupt variations of the thermal boundary conditions as occur there. These difficulties decrease rapidly with distance into the heated region. For example, the data reduction from the experiment did not directly account for the preheating of the air due to upstream conduction and, within 10 diameters, the resulting error of about 1% in $(T_b - T_i)/T_i$ effects the local Nusselt number by about 2% or less [3]. Consequently, comparisons between predictions and measurements are not warranted in the first few diameters of the heated region and Fig. 3 is plotted accordingly.

For the near uniform heat flux region in the range $20 < z/D < 41$ the results provide a similar picture to that from the axial temperature profiles in terms of relative performance. For run 618 the CH, TAS and LS models agree with the data to within about 15% and for run 635 they are within 20% with the LS model clearly being closest. For both these cases the LS model underpredicts the Nusselt number whereas the others overpredict it. For the laminarizing run 445 the LS model is in very close agreement with the experiment and the other two overpredict by about 25%. For both Runs 635 and 445 the JL model improves considerably and joins the CH and TAS models downstream.

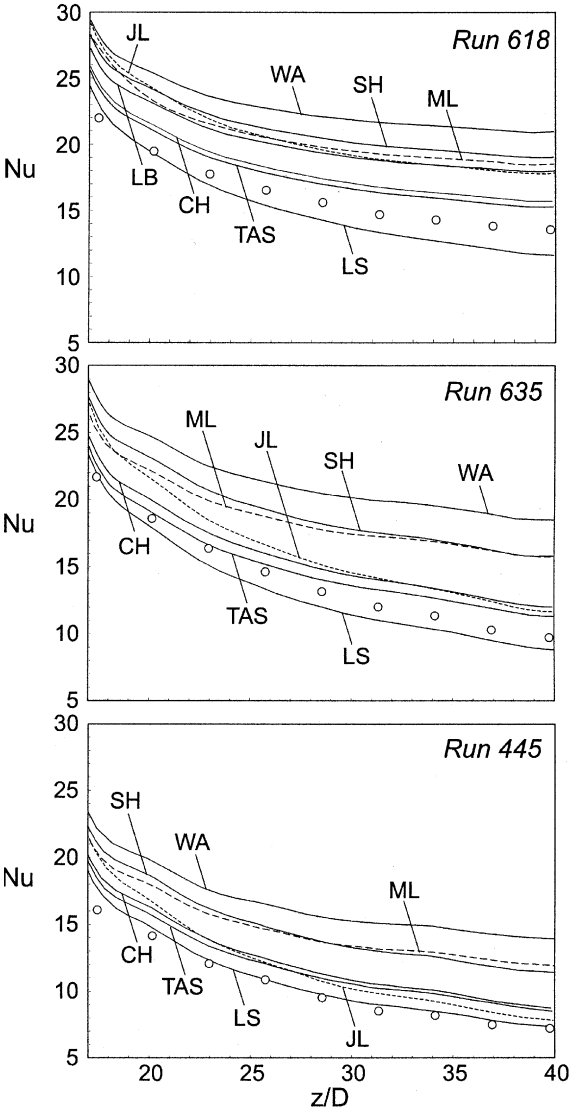

Fig. 3. Variation of local heat transfer parameters as predicted by various turbulence models (lines) and as measured (circles) by Shehata [12].

For all three sets of experimental conditions the Launder and Sharma version performed best; for Runs 635 and 445, its predictions of wall-to-bulk temperature difference differed from the data by less than 6%, which is close to the estimated experimental uncertainty for these conditions. Therefore, in the remainder of this paper results using that model have been selected for comparison with further experimental data (pressure gradients and profiles of local mean velocity and temperature measured at various axial positions). While the wall temperature predictions are probably of main interest to the thermal design engineer, the prediction of pressure drop is also important in the case of the gas flow system

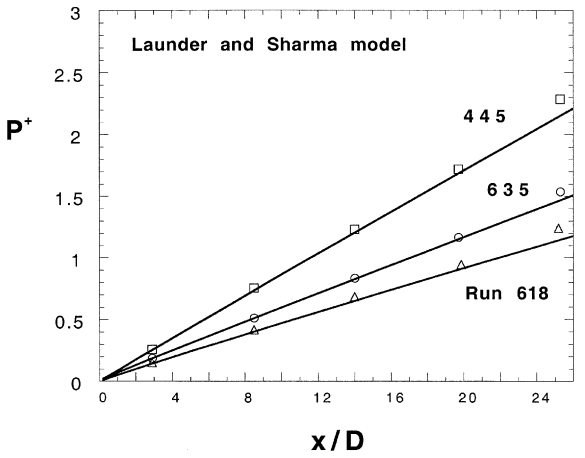

Fig. 4. Effects of heating on non-dimensional pressure defect. Predictions by model of Launder and Sharma [28] and data from Shehata [12].

under consideration here. Fig. 4 demonstrates the close agreement between the values of the non-dimensional pressure decrease P^+ predicted by the Launder–Sharma model and the measurements. Since elevation change and acceleration due to heating are also very significant, this comparison is not a direct verification of the prediction of the wall friction. For run 618 the friction is responsible for only about half of the pressure drop while at the highest heating rate of run 445 it represents only one-third [38]. Consideration of the velocity distributions next gives more evidence on this.

The Launder–Sharma simulations are next assessed in terms of the mean velocity and temperature profiles. Fig. 5(a) and (b) provide direct comparisons between the predicted profiles and the data. Presenting velocities in the form of profiles of W/W_b avoids the uncertainties which would have been involved in the use of u_τ for non-dimensionalization. Presenting temperatures in the form T/T_{in} checks agreement with the energy and mass balances as well as providing a picture of the development of the thermal layer.

In general, the estimated uncertainty in local velocity measurement was calculated to be in the range of 8–10%, with the larger value being associated with measurements near the wall. The uncertainty in local temperature measurement was typically 1% or 2% of the absolute temperature. These estimates are believed to be conservative since comparisons of the integrated and measured total mass flow rates for each profile showed better agreement (3% or less, except near the exit in the runs with the two highest heating rates). In contrast to conventional wisdom, when there is significant *gas* property variation, a mass balance is primarily a test of the profile of the quotient $W\{y\}/T\{y\}$ and an energy balance checks the profile $W\{y\}$ [13].

The measured points nearest the wall correspond to values of y^+ from about 3 to 5, depending on the heating rate and station. The location $y/R = 0.1$ corresponds to $y^+ \approx 20$ for the entry profiles of Runs 618 and 635. At the last station, $y/R = 0.5$ is about $y^+ \approx 60$ and 30 for Runs 618 and 445, respectively. A significant portion of the cross-section is therefore occupied by the viscous layer in all three runs.

The quantity T/T_{in} provides an indication of gas property variation both across and along the tube. In Run 618, T/T_{in} varies by about 50% from the wall to $y/R = 0.5$ at the last station, so μ and k vary by about 40% in that region. In contrast, in run 445 they vary by more than that in the first three diameters of the heated length of the pipe.

At the first station for each run, the velocity *data* points near the wall appear to be high relative to what would be indicated by extrapolation of the data from further out, a common feature in such measurements (and a good reason for not determining u_τ by fitting to $u^+ = y^+$). Measurements at this location required the greatest insertion of the probe support so some aspects of the data reduction are necessarily more uncertain there. In all cases the first *predicted* velocity profiles near the wall are low relative to the data but show good agreement for $y/R > 0.1$; at $x/D \approx 3$, these are the closest to the adiabatic entering turbulent flow. The lower values correspond to lower velocity gradients at the wall and, therefore, lower friction factors; this trend is opposite to that noted for the predictions of adiabatic friction factors.

At the conditions of "turbulent" Run 618, the predicted velocity profiles show reasonable agreement at $x/D \approx 14$ and 25 but are still slightly lower than the data. The lower velocity near the wall implies a lower rate of thermal energy removal by near-wall convection so, with a specified wall heat flux, predicted temperatures near the wall would be high as seen in Fig. 5(b). The corresponding underprediction of local Nusselt numbers is evident in Fig. 3.

The velocity predictions of "intermediate" Run 635 behave much like those of Run 618 with better agreement occurring after the first station, but at $x/D \approx 9$ and 14 the predictions are still low and the temperature predictions are high, accordingly. By 19 diameters the velocity agreement is quite good considering the difficult conditions. Perkins [2] and Torii et al. [10] found that conditions intermediate between turbulent and laminarized were the hardest to predict. Examination in the next section predicts that by $x/D \approx 14$ the flow would be effectively laminarized from the wall to $y/R \approx 0.2$; the temperature profiles near the wall appear laminar as well. While the velocity profile comparison is better at higher axial distances, the temperatures are still overpredicted due to the upstream thermal history, i.e., with the upstream temperature predictions higher than measured,

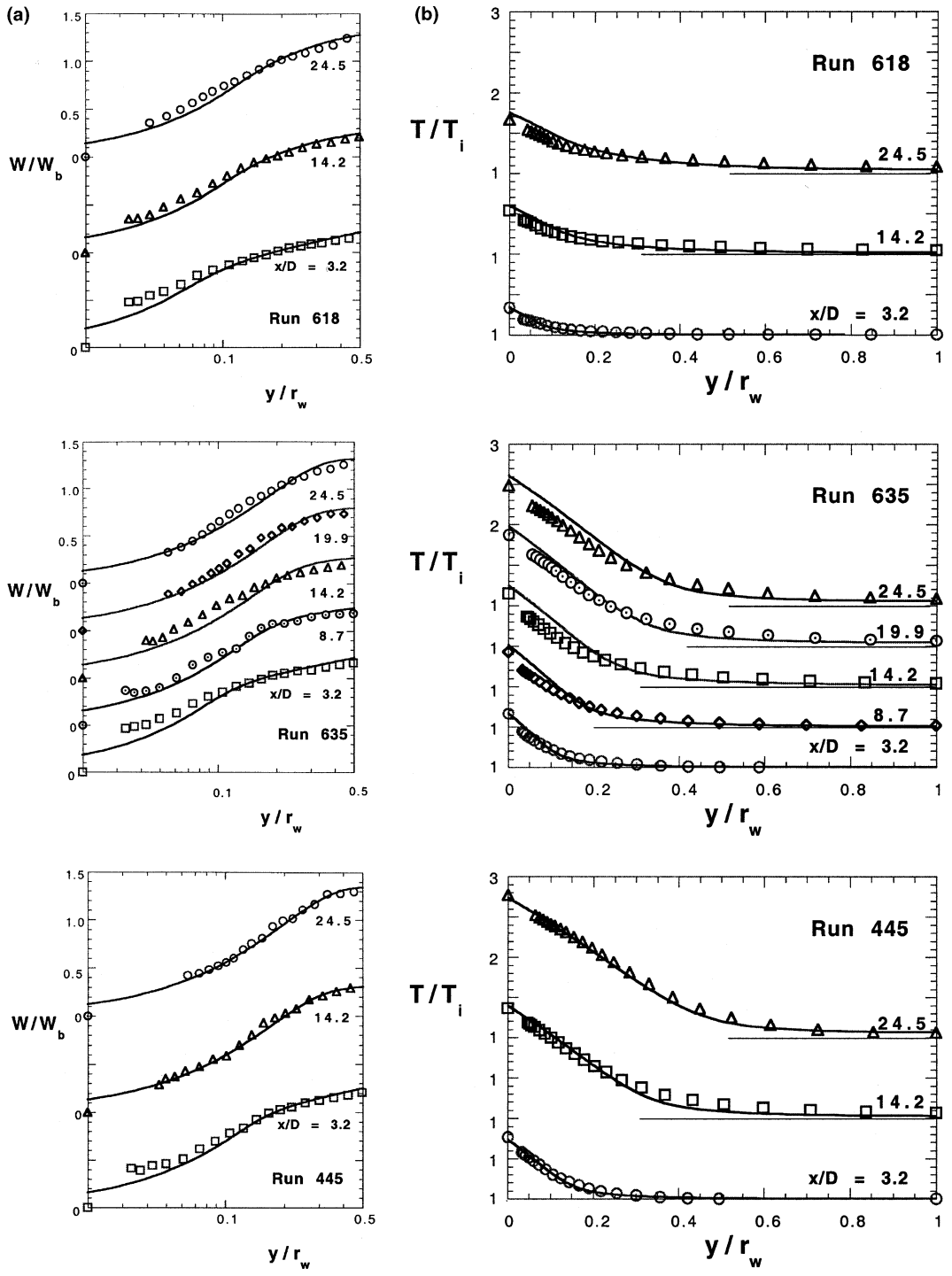

Fig. 5. (a) Predicted axial development of mean streamwise velocity calculated with model of Launder and Sharma [28] (lines) compared to measurements (symbols) of Shehata [12] with strong heating of air in a vertical circular tube. (b) Predicted axial development of mean temperature calculated with the model of Launder and Sharma [28] (lines) compared to the measurements (symbols) of Shehata [12] with strong heating of air in a vertical circular tube.

the simulated thermal layer being convected downstream has more thermal energy. Again these temperatures agree with the development of the wall temperature (Fig. 2) and the trends of $Nu\{x\}$ (Fig. 3).

For Run 445, temperature and velocity predictions generally look good throughout, despite the fluid property variation being greatest for that case. This result probably occurs because molecular transport increases in importance once the laminarizing process has begun and so the uncertainties in the turbulence modeling become of less significance. This explanation is examined further in the later section on the predicted behavior of the Reynolds shear stress.

Overall agreement between the Launder–Sharma predictions and the profile measurements is encouraging though close examination has revealed some detailed discrepancies. In such cases there are corresponding differences between predictions of integral parameters and data. Generally, however, the predictions of velocity and temperature profiles do provide a satisfactory description of the observed behavior.

5. Further discussion of numerical results

5.1. Influences of property variation on integral heat transfer

The need to account properly for gas property variations is demonstrated by the results of further simulations shown in Fig. 6 in terms of the local Nusselt number. For each run the solid line labeled LS F CP presents the result obtained using the Launder–Sharma model with properties held at their inlet values. The dotted line labeled LS B VP is the result using the same model calculated with full property variation, including buoyancy influences. After the first few diameters, the LS B VP predictions agree well with the data as was noted earlier. The discrepancy between the constant property simulations and the data is quite striking. The data show heat transfer deteriorating steadily along the tube in each case. Nusselt numbers fall to values of about 12, 9 and 7 for the "turbulent", "intermediate" and "laminarizing" runs, respectively. The value of 7 in Run 445 is indicative of heat transfer with strongly laminarized flow. In contrast, constant properties predictions develop a fully established heat transfer condition with Nusselt numbers of about 20 for the two higher Reynolds number cases and 15.5 for the lower one. These values are indicative of turbulent flow. The overprediction of heat transfer at the downstream end with the constant properties idealization is about 120% for Run 445.

The question arises as to what extent buoyancy influences were responsible for the deterioration in heat transfer evident in the LS B VP simulations. In order to examine this further calculations were also undertaken with the gravitational body force term suppressed. The results are also presented in Fig. 6, labeled LS F VP. It can be seen that the differences between predictions with and without buoyancy are very small. For the "turbulent" case, Run 618 a slight reduction in Nusselt number is forecast with the inclusion of buoyancy. For the laminarized case, Run 445, a slight increase of the Nusselt number is evident. For the intermediate case, Run 635, almost no difference is seen. Thus, from the simulations it would appear that buoyancy influences were probably not responsible for the deterioration in

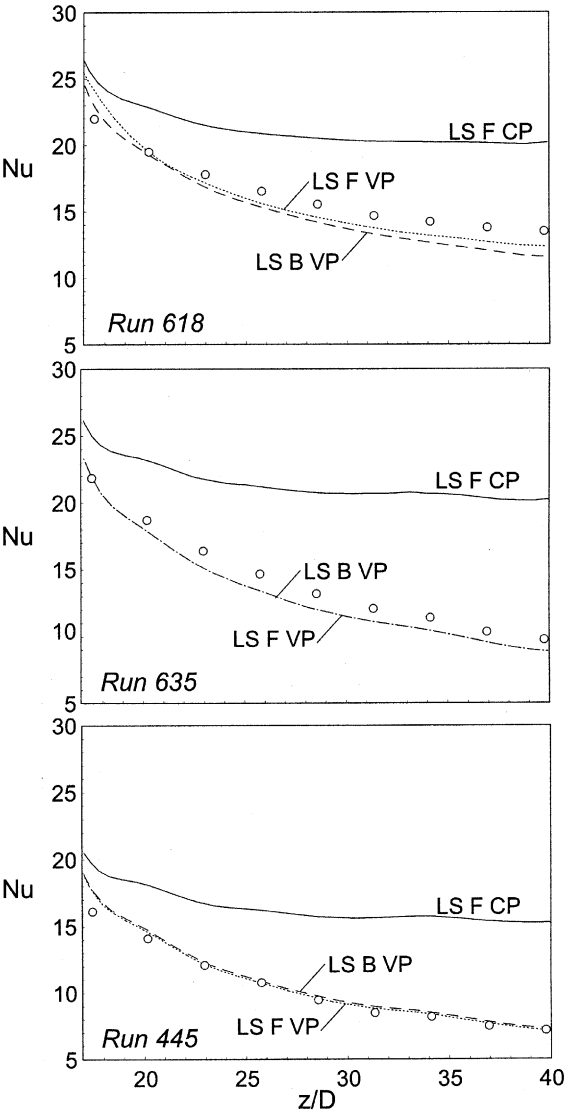

Fig. 6. Forecast effects of buoyancy forces and gas property variation according to the model of Launder and Sharma [28], compared to data of Shehata [12].

heat transfer evident in the experiments under consideration.

Confirmation of this view is provided from evidence from the extensive studies of mixed convection by Jackson et al. [50–53]. For Run 635, their buoyancy parameter B_j ($= Gr_q/Re^{3.425}Pr^{0.8}$) is about 1.6×10^{-6} at the start of heating and about 9×10^{-7} at the last useful station ($x/D \approx 25$). For Run 445, the comparable values are about 5×10^{-6} and 2.4×10^{-6}, respectively. For such values of this parameter, Li [54] found measurable reductions of local Nusselt number due to buoyancy for $x/D > 50$ in his experiments with air flowing upwards in a long uniformly heated tube. However, such reductions were not evident for smaller values of x/D. On this basis it is concluded that, in the view of the comparatively short length of tube used in the experiments under consideration here, measurable buoyancy influences would not be present. The absence of significant buoyancy influences in the present simulations as evidenced by similarity of the LS B VP and the LS F VP simulations is therefore entirely consistent with the above conclusion.

5.2. Further insight concerning buoyancy and acceleration effects

Approximate analyses by Jackson and coworkers [55–57] can provide preliminary insight into the relative effects of acceleration and buoyancy. An order-of-magnitude criterion for the onset of buoyancy effects in developed turbulent pipe flow has been generated by considering modification of the shear stress profile across the viscous layer. Treating properties as constant (with the exception of the affected density) and taking the extent of the affected region as $\delta_{T^+} = \delta_{M^+}/Pr^{0.4}$ with $\delta_{M^+} \approx 26$, Jackson [57] has estimated that for

$$Gr_q/(Re_b^{3.5}Pr^{0.8}) <\sim 5.6 \times 10^{-7}$$

the buoyancy-induced decrease in shear stress across the layer would be less than 10% of the wall shear stress. For a developed turbulent pipe flow, this criterion corresponds approximately to an effect of about 5% on the Nusselt number. That is, below this order-of-magnitude the effect of buoyancy on the heat transfer could be expected to be negligible.

Applying the same reasoning, one can deduce a comparable approximate criterion for the onset of acceleration effects in a pipe flow. From the momentum equation, one approximates

$$\Delta\tau = \tau\{y\} - \tau_w \approx (\mathrm{d}p/\mathrm{d}x)_{\text{equivalent}}\, y \approx -W_b^2(\mathrm{d}\rho_b/\mathrm{d}x)\delta_H$$

In addition to the approximations employed for the buoyancy effect, application of the prefect gas "law" and the energy equation gives

$$(\Delta\tau/\tau_w) \approx (4q^+/Re_b)\delta_{M^+}/((f/2)^{3/2}Pr^{0.4})$$

and an onset criterion of 10% becomes

$$(4q^+/Re_b)(Re_b^{3/8}/Pr^{0.4}) <\sim 2.9 \times 10^{-5}$$

The first parameter is recognized as being approximately equal to the acceleration parameter K_v [7]. For air, this criterion can be transformed to

$$K_v <\sim 9.5 \times 10^{-7} \quad \text{at } Re = 6000$$

and

$$K_v <\sim 1.2 \times 10^{-6} \quad \text{at } Re = 3000$$

For flows accelerated by lateral convergence, Murphy et al. [58] found agreement with turbulent predictions when $K_v <\sim 9.5 \times 10^{-7}$ and agreement with laminar predictions when $K_v >\sim 4 \times 10^{-6}$. With the same apparatus, Chambers et al. [59] observed that the turbulent bursting frequency approached that for fully developed turbulent flow as $K_v \to 10^{-7}$ and approached zero as $K_v \to 4 \times 10^{-6}$. One sees that Jackson's order-of-magnitude analysis is consistent with these experimental observations for accelerated flows.

The relative effects of buoyancy and acceleration can be compared as

$$(\Delta\tau_{\text{buoyancy}}/\Delta\tau_{\text{acceleration}}) \approx (51.6Gr_q/(Re_b^{3.875}Pr^{0.4})) \times (Re_b/(4q^+))$$

For the experiment of Shehata the *highest* values for these criteria can be estimated as in the following table:

Run	Acceleration $(4q^+/Re_b) \times (Re_b^{3/8}/Pr^{0.4})$	Buoyancy $Gr_q/(Re_b^{3.5}Pr^{0.8})$	$\Delta\tau_{buoy}/\Delta\tau_{acc}$
618	3.6×10^{-5}	3.9×10^{-7}–3.1×10^{-7}	0.56–0.46
635	6.6×10^{-5}	7.9×10^{-7}–4.8×10^{-7}	0.61–0.41
445	1.1×10^{-4}	2.5×10^{-6}–1.3×10^{-6}	1.24–0.72

(The higher values are near the thermal entrance.) Thus, for Run 618 both phenomena would be estimated to have only slight effects, with acceleration being more important than buoyancy. If the tube were long, for the other two runs both phenomena might be expected to be significant; for Run 635 both effects could be additive leading to earlier laminarization whereas for Run 445 the implication is that either phenomenon could cause laminarization. However, *since the tube was relatively short, these analyses overestimate the buoyancy effects*. (A more appropriate Grashof number in the thermal entrance might be based on $q''_w\delta_T^4$ which is considerably smaller at low x.)

Available guidance appears contradictory concerning the question whether buoyancy forces should cause significant effects on the heat transfer parameters in

Shehata's flows. At his levels of B_j, Li's [54] combination of his data with a correlation by Petukhov predicts observable and significant reductions of the local Nusselt number. On the other hand, comparison to the thermal entry predictions of Cotton and Jackson [51] indicates small or negligible effects. The differences between these two references include Reynolds number range, approach and gas property variation.

Cotton and Jackson provide predictions for mixed convection with constant fluid properties, emphasizing buoyancy effects. For ascending flow of gases at $Re = 5000$, they found marked development effects (their Fig. 2); at $z/D = 10$, they predict a maximum reduction of Nusselt number of only 10% regardless of heating rate. For $z/D = 20$, they forecast a reduction of 10% at $B_j \approx 2.5 \times 10^{-6}$ with a value of about 5×10^{-6} required for a reduction of 20%. Apparently the thermal boundary layer must first grow sufficiently for the buoyant force to act over a large enough region to affect the convective heat transfer. Thus, another possible benefit of the "short" heated section in Shehata's experiment could be retaining the desired condition of dominant forced convection while obtaining significant variation of fluid properties.

In ascending *laminar* flow, significant buoyancy effects initially induce increased velocity gradients and velocities near the wall; a blunt velocity profile evolves as for a favorable pressure gradient or streamwise accelerating flow. Consequences are increased stability (retarding transition) and higher velocities which improve convective heat transfer as shown by Worsoe-Schmidt and Leppert [60] and Jackson et al. [50].

There are only a few experimental results available with significant property variation and low Reynolds numbers that provide direct comparisons of mixed convection versus forced convection at the same conditions. Bates et al. [61] obtained three sets of data by increasing the gas pressure while holding mass flow rate and heating rate constant: "turbulent", "slow laminarization" and "rapid laminarization". (Vilemas et al. [62] also varied gas pressure but did not present direct comparisons with the other quantities held constant.) For "rapid laminarization", increasing the buoyancy parameter gave a slight enhancement, as would be expected for laminar flow. For "slow laminarization", with initial conditions of $Re_i \approx 5840$, $q_i^+ \approx 0.0031$, $|Gr/Re_i^2| \approx 0.23$ and $B_{ji} \approx 1.3 \times 10^{-6}$ for the higher pressure run, there was a reduction in Nusselt number of about 8% at $z/D \approx 25$; these parameters were in about the same range as Shehata's run 635. Their "turbulent" run ($Re_i \approx 6900$, $q_i^+ \approx 0.0010$, $|Gr/Re_i^2| \approx 0.45$ and $B_{ji} \approx 2.0 \times 10^{-6}$) had higher Reynolds numbers and buoyancy parameters with a lower heating rate than the present calculations and measurements for run 618—and it showed a 25% reduction in Nusselt number due to buoyancy influences.

Based on the relation of the Bates et al. results to those of Li, one may estimate that the effects of buoyancy forces at the conditions of Shehata's experiments could be of the following order:

Run 618	$x/D \approx 11$	$\Delta Nu/Nu_{fc}$	$\approx 2\%$
	$x/D \approx 25$		$<\sim 5\%$
Run 635	$x/D \approx 11$		$<\sim 5\%$
	$x/D \approx 25$		$<\sim 7\%$
Run 445	Laminarizing, probably negligible or slight enhancement		

However, since numerical predictions of the Reynolds stresses and turbulent heat fluxes forecast that Run 635 begins to laminarize near the end of the test section, it may have less change due to buoyancy forces than suggested in this table. Lacking comparisons based on direct measurements, one must consider these estimates to be somewhat speculative.

Two messages evolve from this consideration of buoyancy effects. First, there remains need for careful measurements directly comparing forced and mixed convection for a greater range of low Reynolds number flows with significant heating; it could be a simple experiment, as demonstrated by Bates et al., but it is considered to be beyond the scope of the present study. Secondly, forced convection dominates the heat transfer results at the conditions of Shehata's experiment. We estimate that buoyancy would have affected the Nusselt number by 7% or less in the worst case.

5.3. Influence of intense heating on turbulence

Since the model of Launder and Sharma performed better than the others in forecasting wall temperatures and Nusselt numbers for the conditions of the experiment, and also reproduced the profiles of local mean velocity and temperature satisfactorily, we next examine its predictions of turbulence quantities.

Predicted profiles of the normalized *turbulent viscosity* (μ_t/μ) plotted against normalized distance from the wall are shown in Fig. 7. These demonstrate the growth of the viscous layer, the region near the wall where turbulent viscosity is small compared with molecular viscosity. The rate at which this happens with change of axial location increases with q^+. As a measure of an effective *viscous layer thickness*, say δ, we can choose the distance from the wall where $(\mu_t/\mu) \approx 1$. For conditions where $Re_{in} \approx 6000$ (Runs 618 and 635) $\delta/R \approx 0.06$ at the inlet where as for $Re_{in} \approx 4300$ it is about 0.09 (Run 445). By the last measurement station, δ/R is predicted to grow to about 0.18, 0.42 and 0.53 for "conditions" 618, 635 and 445, respectively. These predictions are entirely consistent with the explanation offered earlier by one of the present authors that the cause of the unexpected reduction in effectiveness of heat transfer in strongly

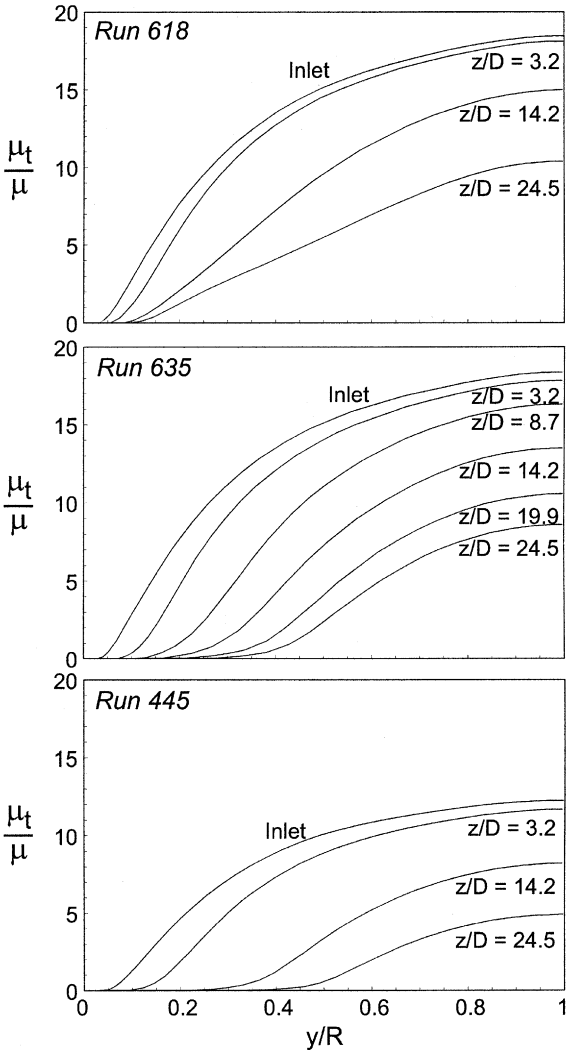

Fig. 7. Predictions of axial development of turbulent viscosity for conditions of experiments by Shehata [12] calculated with model of Launder and Sharma [28].

heated pipe flow was thickening of the viscous sublayer [1, p. 131].

In the heated region, the effective viscous layer thickness for Run 618 is forecast to increase by a factor of about three and the centerline value of (μ_t/μ) is expected to decrease by a factor of about two. However, the resulting profiles of *Reynolds stress* (see Fig. 8a) retain the shape of a turbulent shear stress profile corresponding to a reduced Reynolds number and wall shear stress. The peak value of the Reynolds stress at $x/D \approx 25$ is about half that for the inlet profile and it occurs slightly further from the wall; thus, the normalized profile τ_t/τ_w is approximately self-preserving away from the wall.

Predictions for Run 635 show lower values than Run 618 at equivalent stations. For example, at the last station and $y/R = 0.2$, the Reynolds stress profile for Run 618 is only about half that of the entry profile whereas for 635 the corresponding profile is forecast to decrease by a factor of about twenty. Peak values are correspondingly lower. Thus, run 635 shows significantly less turbulent momentum transport than run 618, which is considered to be representative of gas flow with property variation that retains its turbulent character. In that sense, run 635 is predicted to be almost laminarized.

Expectations were that for Run 445 suppression of turbulent transport might be more extreme than for Run 635. The calculations forecast continuous thickening of the viscous-dominated region and reduction in the maximum values of the Reynolds stresses. The contribution of turbulent transport is predicted to be significantly decreased as axial distance increases. For example, within 14 diameters the maximum Reynolds stress decreases by about an order-of-magnitude from its value at the inlet. At $x/D \approx 25$, the maximum Reynolds stress is predicted by the model of Launder and Sharma to be near zero for these conditions.

For a slightly higher heating rate ($q^+ \approx 0.0055$), Perkins [2] predicted the development of the mean temperature profile well using a very simple model in which turbulent transport was neglected. In his approach, *turbulent* entering velocity profiles were specified and then the governing equations were solved with turbulent viscosity and turbulent thermal conductivity both set to zero throughout the thermal entry region. The present predictions of the development of the turbulent shear stress for Run 445 demonstrate why Perkins's approach could be successful at high heating rates; these turbulent transport quantities are forecast to become negligible quickly after the application of strong heating.

While the predictions of Runs 635 and 445 suggest very much reduced turbulent momentum transfer rates by the end of the heated region, the turbulent viscosity profiles imply that there could still be turbulent fluctuations in the core region of the flow. For both of these runs, the profiles showing the development of μ_t/μ (Fig. 7) could be thought of in terms of a laminar boundary layer growing into a turbulent freestream flow (the core region). For k–ε models, the turbulent viscosity is related to k and ε by $\mu_t = C_\mu f_\mu \rho k^2/\bar{\varepsilon}$. The value of μ_t/μ would correspond to significant turbulent kinetic energy at the centerline (unless $\bar{\varepsilon}$ is very low); Fig. 8b demonstrates that the numerical predictions of *turbulent kinetic energy* are consistent with this idea.

The simulations predict that the turbulence kinetic energy would decrease axially for all three conditions. For run 618 the profile maintains its typical shape as expected for turbulent flow in a circular tube. Most of the reduction occurs in the first 14 diameters and then

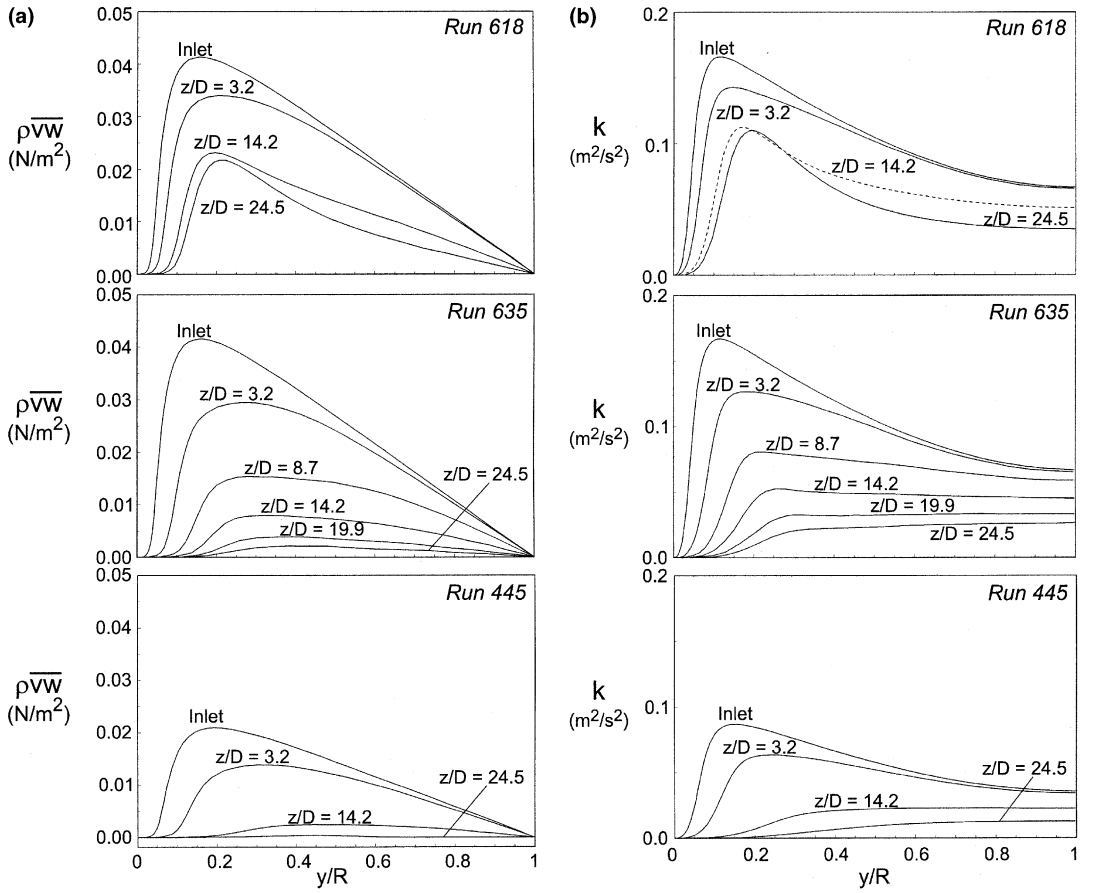

Fig. 8. Predictions of axial development of turbulence quantities calculated with model of Launder and Sharma [28] for conditions of experiments by Shehata [12]: (a) Reynolds stresses and (b) turbulence kinetic energy.

the decrease is not as severe. Runs 635 and 445 show a gradual transition from this typical turbulent shape at the entry to a monotonically increasing profile from wall to centerline at the end of the heated section. This transition occurs at shorter distances for the higher heating rate and lower Reynolds number; for example, at $x/D \approx 14$ one sees a difference in predicted shapes. At $x/D \approx 25$ the diffusive (gradient) transport of turbulence kinetic energy would be solely from the centerline towards the wall, with negligible production at the centerline ($\partial W/\partial y = 0$ by symmetry). The situation involves the gradual decay of pre-existing turbulence. So, while laminarization is clearly being forecast, a hot wire sensor at the centerline would still show turbulent fluctuations at this location, as observed by Bankston [63] and Ogawa et al. [64].

6. Concluding remarks

A number of turbulence models, developed for turbulent flows under conditions of uniform fluid properties, have been used in a computational study for the purposes of simulating experiments with strongly heated, variable property gas flows at low Reynolds numbers in a vertical circular tube [12]. The selection of models included a mixing length model, eddy diffusivity models, a one-equation k model and two-equation models of k–ε type with low-Reynolds-number treatments; this selection is representative of models which have been widely used is but not all-inclusive. Thermal energy transport was modeled using a turbulent Prandtl number.

New knowledge developed includes confirmation that a particular model can be directly extended to simulate the internal mean distributions of strongly heated flows usefully, insight into the effects leading to laminarization and how they relate to the model and observation of the behavior of the simulated turbulent shear stress which leads to validated predictions of internal velocity and temperature fields.

For the purpose of making a preliminary assessment of the models, predictions of the friction factor and Nusselt number were made using them for fully

established flow and heat transfer in a tube for air at low Reynolds numbers under conditions of constant properties. The results were compared with values given by well established empirical equations. Only one model gave Nusselt numbers which agreed with the empirical values within their estimated uncertainties. This was the low-Reynolds-number k–ε model of Launder and Sharma [28]. Several k–ε models which were specifically developed for low-Reynolds-number applications gave unacceptably high results.

Turning next to the variable property predictions, one sees the experiments simulated involved heating rates which were varied so as to cause significant influences on turbulence, in some cases leading to laminarization. The apparatus was a vertical circular tube with an unheated entry length for flow development, followed by a resistively heated section which provided a thermal boundary condition of approximately uniform wall heat flux. Inlet Reynolds numbers of 6080, 6050 and 4260 with non-dimensional heating rates, $q^+ = q''_w/(Gc_pT_i)$, of about 0.0018, 0.0035 and 0.0045, respectively, were employed. The parameters were chosen with a view to the conditions being predominantly those of forced convection. Profiles of mean velocity and temperature were measured using hot wire anemometry.

Simulations of the experiments were made using eight turbulence models. These provided predictions of integral heat transfer parameters for comparison with experiment. The resulting axial wall temperature distributions and Nusselt numbers for eight models were compared to the data from the three runs. At the location where the wall temperature was highest, the wall-to-bulk temperature difference was underpredicted by up to 40% by some of the low-Reynolds-number k–ε models. For all three sets of experimental conditions the Launder–Sharma model gave the best results: for the two higher heating rates, its predictions of temperature difference differed from the data by only 6%, which is comparable to the estimated experimental uncertainty of the measurements for these conditions. Furthermore, the Launder–Sharma predictions of mean velocity and temperature profiles proved to be in good overall agreement with the measured profiles. It is therefore concluded that the predicted turbulence quantities should provide useful insight into the influences present in the experiment.

Examination of the predicted Reynolds stress and turbulent viscosity suggests that the run at the lowest heating rate behaves as a turbulent flow, but with some reduction in turbulent transport near the wall. For the higher heating rates, the predicted turbulence quantities showed a steady decline in the viscous layer region with increased axial position—representative of conditions which might be described as laminarizing. Overall, the agreement between the predictions of mean velocity and temperature profiles and the data was good.

Acknowledgements

The study reported was supported by the University of Manchester, by the Nuclear Energy Research Initiative of the US Department of Energy and by the Long Term Research Initiative Program of the Idaho National Engineering and Environmental Laboratory under DoE Idaho Field Office Contracts DE-AC07-94ID13223 and DE-AC07-99ID13727. The experiments of Dr. Shehata were funded by the Office of Naval Research, the National Science Foundation and the University of Arizona. To all we are extremely grateful. By acceptance of this article for publication, the publisher recognizes the US Government's (license) rights in any copyright and the Government and its authorized representatives have unrestricted right to reproduce in whole or in part said article under any copyright secured by the publisher.

References

[1] D.M. McEligot, The effect of large temperature gradients on turbulent flow of gases in the downstream region of tubes, Ph.D. thesis, Stanford University, 1963. Also TID-19446.

[2] K.R. Perkins, Turbulence structure in gas flows laminarizing by heating, Ph.D. thesis, University of Arizona, 1975.

[3] A.M. Shehata, D.M. McEligot, Mean turbulence structure in the viscous layer of strongly-heated internal gas flows. Measurements, Int. J. Heat Mass Transfer 41 (1998) 4297–4313.

[4] D.M. McEligot, Convective heat transfer in internal gas flows with temperature-dependent properties, Adv. Transport Processes 4 (1986) 113–200.

[5] C.A. Bankston, D.M. McEligot, Turbulent and laminar heat transfer to gases with varying properties in the entry region of circular ducts, Int. J. Heat Mass Transfer 13 (1970) 319–344.

[6] S.J. Kline, W.C. Reynolds, F.A. Schraub, P.W. Rundstadler, The structure of turbulent boundary layers, J. Fluid Mech. 30 (1967) 741–773.

[7] D.M. McEligot, C.W. Coon, H.C. Perkins, Relaminarization in tubes, Int. J. Heat Mass Transfer 9 (1970) 1151–1152.

[8] H. Kawamura, Analysis of laminarization of heated turbulent gas using a two-equation model of turbulence, in: Proceedings of the Second International Symposium on Turbulent Shear Flow, London, 1979, pp. 18.16–18.21.

[9] S. Fujii, N. Akino, M. Hishida, H. Kawamura, K. Sanokawa, Experimental and theoretical investigations on heat transfer of strongly heated turbulent gas flow in an annular duct, JSME Int. J., Ser. II 34 (3) (1991) 348–354.

[10] S. Torii, A. Shimizu, S. Hasegawa, M. Higasa, Numerical analysis of laminarizing circular tube flows by means of a Reynolds stress turbulence model, Heat Transfer—Jpn. Res. 22 (1993) 154–170.

[11] S. Torii, W.-J. Yang, Laminarization of turbulent gas flow inside a strongly heated tube, Int. J. Heat Mass Transfer 40 (1997) 3105–3117.
[12] A.M. Shehata, Mean turbulence structure in strongly heated air flows, Ph.D. thesis, University of Arizona, 1984.
[13] A.M. Shehata, D.M. McEligot, Turbulence structure in the viscous layer of strongly heated gas flows. Tech. report INEL-95/0223, Idaho National Engineering Laboratory, 1995.
[14] D.P. Mikielewicz, Comparative studies of turbulence models under conditions of mixed convection with variable properties in heated vertical tubes, Ph.D. thesis, University of Manchester, 1994.
[15] M.A. Cotton, Theoretical studies of mixed convection in vertical tubes, Ph.D. thesis, University of Manchester, 1987.
[16] L.S.L. Yu, A computational study of turbulent mixed convection in vertical tubes, Ph.D. thesis, University of Manchester, 1991.
[17] S. Wisniewski, Wymiana ciepla, PWN, Warsawa, 1988 (in Polish).
[18] B.E. Launder, D.B. Spalding, Lectures on mathematical models of turbulence, Academic Press, London, 1972.
[19] W.M. Kays, M.E. Crawford, Convective heat and mass transfer, third ed., McGraw-Hill, New York, 1993.
[20] J. Nikuradse, Gesetzmassigkeit der turbulenten Strömung in glatten Rohren. Forschungsheft 356, 1932. Also Project SQUID Rpt. TM-PUR-11, Purdue University, August 1949.
[21] E.R. van Driest, On turbulent flow near a wall, J. Aerospace Sci. 23 (1956) 1007–1011 and 1036.
[22] H. Reichardt, Complete representation of a turbulent velocity distribution in smooth tubes, Z. Angew. Math. Mech. 31 (1951) 208–219.
[23] R.G. Deissler, Analysis of turbulent heat transfer, mass transfer and friction in smooth pipes at high Prandtl and Schmidt number. NACA Report 1210, 1955.
[24] M. Wolfshtein, The velocity and temperature distribution in one-dimensional flow with turbulence augmentation and pressure gradient, Int. J. Heat Mass Transfer 12 (1969) 301–318.
[25] B.P. Axcell, W.B. Hall, Mixed convection of air in a vertical pipe. Heat Transfer 1978, Proceedings of the Sixth International Heat Transfer Conference, Toronto, vol. 1, Paper MC-7, 1978, pp. 37–42.
[26] W.P. Jones, B.E. Launder, The prediction of laminarization with a two-equation model of turbulence, Int. J. Heat Mass Transfer 15 (1972) 301–314.
[27] W.P. Jones, B.E. Launder, The calculation of low-Reynolds-number phenomena with a two-equation model of turbulence, Int. J. Heat Mass Transfer 16 (1973) 1119–1130.
[28] B.E. Launder, B.I. Sharma, Application of the energy-dissipation model of turbulence to the calculation of flow near a spinning disc, Lett. Heat Transfer 1 (1974) 131–138.
[29] K.Y. Chien, Predictions of channel and boundary-layer flows with a low-Reynolds-number turbulence model, AIAA J. 20 (1982) 33–38.
[30] C.K.G. Lam, K.A. Bremhorst, Modified form of the k–ε model for predicting wall turbulence, J. Fluids Engng. 103 (1981) 456–460.
[31] V. Michelassi, W. Rodi, G. Scheuerer, Testing a low-Reynolds-number k–ε turbulence model based on direct simulation data. U. Karlsruhe manuscript presented at Eighth Symposium on Turbulent Shear Flows, München, 1991 (not included in pre-printed proceedings).
[32] T.H. Shih, A.T. Hsu, An improved k–ε model for near-wall turbulence. AIAA paper 91-0611, 1991.
[33] S. Thangam, R. Abid, C.G. Speziale, Application of a new k–τ model to near wall turbulent flows, AIAA J. 30 (1992) 552–554.
[34] M. Nishimura, S. Fujii, A.M. Shehata, T. Kunugi, D.M. McEligot, Prediction of forced gas flows in circular tubes at high heat fluxes, J. Nucl. Sci. Technol. (Atomic Energy Society of Japan) 37 (2000) 581–594.
[35] R.A. Antonia, J. Kim, Turbulent Prandtl number in the near-wall region of a turbulent channel flow, Int. J. Heat Mass Transfer 34 (1991) 1905–1908.
[36] D.M. McEligot, C.A. Bankston, Turbulent predictions for circular tube laminarization by heating. ASME paper 69-HT-52, 1969.
[37] D.M. McEligot, P.E. Pickett, M.F. Taylor, Measurement of wall region turbulent Prandtl numbers in small tubes, Int. J. Heat Mass Transfer 19 (1976) 799–803.
[38] K. Ezato, A.M. Shehata, T. Kunugi, D.M. McEligot, Numerical predictions of transitional features of turbulent gas flows in circular tubes with strong heating, J. Heat Transfer 121 (1999) 546–555.
[39] B.P. Axcell, The effect of buoyancy on forced convection heat transfer, Ph.D. thesis, University of Manchester, 1975.
[40] D.C. Wilcox, Reassessment of the scale-determining equation for advanced turbulence models, AIAA J. 26 (1988) 1299–1310.
[41] M.A. Leschziner, An introduction and guide to the computer code PASSABLE. Report, Mech. Engr. Dept., UMIST, 1982.
[42] G.D. Raithby, G.E. Schneider, Numerical solution of problems in incompressible fluid flow: treatment of velocity–pressure coupling, Numer. Heat Transfer 2 (1979) 417–440.
[43] P.J. Kirwin, Investigation and development of two-equation turbulence closures with reference to mixed convection in vertical pipes, Ph.D. thesis, University of Manchester, 1995.
[44] B.E. Launder, C.H. Priddin, A comparison of some proposals for the mixing length near a wall, Int. J. Heat Mass Transfer 16 (1973) 700–702.
[45] V.C. Patel, W. Rodi, G. Scheurer, Turbulence models for near-wall and low Reynolds number flows: a review, AIAA J. 23 (1985) 1308–1319.
[46] F.W. Dittus, L.M.K. Boelter, Heat transfer in automobile radiators of the tubular type, in: Pub. in Engrg., 2, University of California, Berkeley, 1930, pp. 443–461.
[47] W.H. McAdams, Heat Transmission, third ed., McGraw-Hill, New York, 1954, p. 219.
[48] D.M. McEligot, L.W. Ormand, H.C. Perkins, Internal low Reynolds number turbulent and transitional gas flow with heat transfer, J. Heat Transfer 88 (1966) 239–245.
[49] B.S. Petukhov, V.A. Kurganov, A.I. Gladuntsov, Turbulent heat transfer in tubes to gases with variable physical properties, Heat and Mass Transfer 1 (1972) 117–127, Izd. ITMO AN BSSR, Minsk (in Russian).

[50] J.D. Jackson, M.A. Cotton, B.P. Axcell, Studies of mixed convection in vertical tubes, Int. J. Heat Fluid Flow 10 (1989) 2–15.
[51] M.A. Cotton, J.D. Jackson, Vertical tube air flows in the turbulent mixed convection regime calculated using a low-Reynolds-number k–ε model, Int. J. Heat Mass Transfer 33 (1990) 275–286.
[52] J.D. Jackson, J. Li, Numerical simulations of variable property, buoyancy-influenced turbulent convection in a heated tube, in: P.A. Thibault, D.M. Bergeron (Eds.), CFD 95, Proceedings of the Third Annual Conference, vol. II, CFS Society Canada, Banff, 1995, pp. 251–257.
[53] J. Li, J.D. Jackson, Buoyancy-influenced variable property turbulent heat transfer to air flowing in a uniformly heated vertical tube, Proceedings, Engineering Foundation Second International Conference on Turbulent Heat Transfer, Manchester, June 1998.
[54] J.K. Li, Studies of buoyancy-influenced convective heat transfer to air in a vertical tube, Ph.D. thesis, University of Manchester, 1994.
[55] W.B. Hall, J.D. Jackson, Laminarization of a pipe flow by buoyancy forces, ASME paper 69-HT-55, 1969.
[56] J.D. Jackson, W.B. Hall, Influences of buoyancy on heat transfer of fluids flowing in vertical tubes under turbulent conditions, in: S. Kakac, D.B. Spalding (Eds.), Turbulent Forced Convection in Channels and Bundles, vol. 2, Hemisphere, Washington, 1979, pp. 613–640.
[57] J.D. Jackson, Personal communication, University of Manchester, April 1998.
[58] H.D. Murphy, F.W. Chambers, D.M. McEligot, Laterally converging flow. I. Mean flow, J. Fluid Mech. 127 (1983) 379–401.
[59] F.W. Chambers, H.D. Murphy, D.M. McEligot, Laterally converging flow. II. Temporal wall shear stress, J. Fluid Mech. 127 (1983) 403–428.
[60] P.M. Worsoe-Schmidt, G. Leppert, Heat transfer and friction for laminar flow of a gas in a circular tube at high heating rate, Int. J. Heat Mass Transfer 8 (1965) 1281–1301.
[61] J.A. Bates, R.A. Schmall, G.A. Hasen, D.M. McEligot, Effects of buoyant body forces on forced convection in heated laminarizing flows, in: Heat Transfer 1974, Fifth International Heat Transfer Conference, Tokyo, vol. 2, 1974, pp. 141–145.
[62] J.V. Vilemas, P.S. Poskas, V.E. Kaupas, Local heat transfer in a vertical gas-cooled tube with turbulent mixed convection and different heat fluxes, Int. J. Heat Mass Transfer 35 (1992) 2421–2428.
[63] C.A. Bankston, The transition from turbulent to laminar gas flow in a heated pipe, J. Heat Transfer 92 (1970) 569–579.
[64] M. Ogawa, H. Kawamura, T. Takizuka, N. Akino, Experiment on laminarization of strongly heated gas flow in a circular tube, J. Atomic Energy Soc., Japan 24 (1) (1982) 60–67 (in Japanese).